

Using computed muscle control to generate forward dynamic simulations of human walking from experimental data

Darryl G. Thelen^{a,*}, Frank C. Anderson^b

^a*Department of Mechanical Engineering, University of Wisconsin-Madison, Madison, WI, USA*

^b*Biomechanical Engineering Division, Mechanical Engineering Department, Stanford University, Stanford, CA, USA*

Accepted 8 February 2005

Abstract

The objective of this study was to develop an efficient methodology for generating muscle-actuated simulations of human walking that closely reproduce experimental measures of kinematics and ground reaction forces. We first introduce a residual elimination algorithm (REA) to compute pelvis and low back kinematic trajectories that ensure consistency between whole-body dynamics and measured ground reactions. We then use a computed muscle control (CMC) algorithm to vary muscle excitations to track experimental joint kinematics within a forward dynamic simulation. CMC explicitly accounts for delays in muscle force production resulting from activation and contraction dynamics while using a general static optimization framework to resolve muscle redundancy. CMC was used to compute muscle excitation patterns that drove a 21-degrees-of-freedom, 92 muscle model to track experimental gait data of 10 healthy young adults. Simulated joint kinematics closely tracked experimental quantities (mean root-mean-squared errors generally less than 1°), and the time histories of muscle activations were similar to electromyographic recordings. A simulation of a half-cycle of gait could be generated using approximately 30 min of computer processing time. The speed and accuracy of REA and CMC make it practical to generate subject-specific simulations of gait.

© 2005 Elsevier Ltd. All rights reserved.

Keywords: Musculoskeletal modeling; Dynamic simulation; Optimization; Control; Gait

1. Introduction

Forward dynamic simulation offers a potentially powerful methodology for characterizing the causal relationship between muscle excitations and multi-joint movement during gait. For example, recent studies have used simulations of normal walking to quantify the contributions of lower extremity muscles to vertical support, forward progression, and swing leg kinematics (Neptune et al., 2001; Anderson and Pandey, 2003; Anderson et al., 2004; Goldberg et al., 2004; Neptune et al., 2004). Unfortunately, conventional approaches for generating dynamic simulations of gait require inordi-

nate amounts of computation time (Anderson and Pandey, 2001; Neptune et al., 2001) making the widespread use of forward dynamic simulation, particularly on a subject-specific basis, impractical.

Computed muscle control (CMC) is a new approach for generating forward dynamic simulations that offers substantial performance benefits over conventional dynamic optimization techniques. Dynamic optimization typically require thousands of complete integrations of the model state equations to converge to a solution (Neptune, 1999; Anderson and Pandey, 2001), which translates into days, weeks or even months of computer time depending on the complexity of the model. Even then, numerical difficulties are endemic to dynamic optimization of complex nonlinear problems, which can lead to sub-optimal solutions (Neptune, 1999). In contrast, CMC, by employing feedforward and feedback

*Corresponding author. Tel.: +1 608 262 1902;
fax: +1 608 265 2316.

E-mail address: thelen@engr.wisc.edu (D.G. Thelen).

control, is able to closely track experimental kinematics using only a single integration of the model state equations. We previously demonstrated that CMC could generate an accurate, coordinated simulation of bicycle pedaling with less than 10 min of computer processing time (Thelen et al., 2003).

CMC is well suited for simulating movements in which all degrees-of-freedom can be independently controlled via muscle actions. However, during gait, the motion of the center-of-mass is dictated by intermittent foot–floor reaction forces. While both foot–floor forces and whole-body motion can be recorded experimentally, they generally are not dynamically consistent due to measurement errors and modeling assumptions (Vaughan et al., 1982; Kuo, 1998; Cahouet et al., 2002). As a result, it is not possible to use CMC to vary muscle excitations to drive a forward dynamic model to replicate both experimental kinematic and kinetic measures without the application of additional external forces, often referred to as residual forces. Furthermore, the original formulation of CMC did not explicitly account for delays in force production due to muscle activation and muscle–tendon contraction dynamics. Although the motions of the body segments are relatively slow during gait, ground reaction forces do change rapidly during loading and push off. As a consequence, failure to account for delays involved in the production of muscle forces can lead to substantial tracking errors.

The objective of this study was to develop a methodology for efficiently generating simulations of human walking that closely track experimental measures of body kinematics and ground reaction forces without the application of residual forces. In this paper, we first describe a technique for ensuring consistency between whole-body dynamics and measured ground reaction forces. We then introduce a modified version of CMC that explicitly accounts for delays in muscle force production. This approach is shown to generate accurate subject-specific forward simulations of normal gait with relatively little computer processing time.

2. Methods

2.1. Forward dynamic musculoskeletal model

The body was modeled as an 8-segment, 21-degree-of-freedom articulated linkage actuated by 92 Hill-type muscle–tendon units. Major aspects of this musculoskeletal model have been described elsewhere (Delp et al., 1990; Delp and Loan, 2000) and previously used to reproduce the salient features of normal gait in the sagittal, transverse, and frontal planes (Anderson and Pandy, 2001). The coupling of muscle excitation (u) to activation (a) was modeled as a first-order process with

rise and decay time constants of 10 and 40 ms, respectively (Zajac, 1989). Musculotendon contraction dynamics were described by a lumped-parameter model that accounts for the interaction of the force–length–velocity properties of muscle and the elastic properties of tendon (Zajac, 1989; Schutte et al., 1993). The model controls (\bar{u} , individual muscle excitation levels) were allowed to vary continuously between zero (no excitation) and one (full excitation).

The generalized coordinates (\bar{q}) of the model correspond to the 21 independent degrees-of-freedom of the system:

$$\bar{q} = \{\bar{q}_x \ \bar{q}_p \ \bar{q}_r \ \bar{q}_l \ \bar{q}_b\}^T, \quad (1)$$

where \bar{q}_x is the translational position of the pelvis, \bar{q}_p are body-fixed Z – X – Y rotation angles describing the pelvis orientation, \bar{q}_r and \bar{q}_l are 6×1 vectors of the joint angles of the right and left limb, and \bar{q}_b is a vector of low back angles describing successive flexion/extension, lateral bending, and transverse rotations, and the superscript T indicates the transpose of the vector. The limb joint angles included three rotations to describe the orientation of the femur relative to the pelvis, a knee flexion angle that governs tibiofemoral and patellofemoral kinematics in the sagittal plane (Yamaguchi and Zajac, 1989), and rotation angles about the ankle and subtalar joint axes.

The accelerations of the generalized coordinates of the model, $\bar{\ddot{q}}$, are dictated by the system equations of motion:

$$\begin{aligned} \vec{M}(\bar{q}) \cdot \bar{\ddot{q}} + \vec{C}(\bar{q}, \dot{\bar{q}}) + \vec{G}(\bar{q}) \\ = \begin{bmatrix} \vec{0}_{6 \times n} \\ \vec{R}_m(\bar{q}) \end{bmatrix} \cdot \vec{f}_m + \vec{R}_{\text{grf}}(\bar{q}) \cdot \vec{f}_{\text{grf}}, \end{aligned} \quad (2)$$

where $\dot{\bar{q}}$ are the generalized speeds, \vec{M} is the system mass matrix, \vec{G} is a vector of generalized forces due to gravity, \vec{C} is a vector of generalized forces arising from Coriolis and centripetal forces, $\vec{0}_{6 \times n}$ is a matrix of zeros signifying that muscles forces do not directly actuate the position or orientation of the pelvis, \vec{R}_m is a matrix of the muscle moment arms about the anatomic joints, n is the number of muscles, \vec{f}_m is a vector of muscle forces and \vec{R}_{grf} is a matrix that transforms the resultant ground reactions, \vec{f}_{grf} , to generalized forces acting on the system.

2.2. Residual elimination algorithm

We used a residual elimination algorithm (REA) to compute pelvis translations and low back angles that

eliminate the need for residual forces. This was accomplished using the overall equations of motion (first 6 equations of (2)) which are independent of muscle forces and require that the net external forces balance the sum of forces and torques due to coriolis, centripetal, gravitational and inertial effects (Greenwood, 1988). These equations were solved for the pelvis translational accelerations (\ddot{q}_x) and low back angular accelerations (\ddot{q}_b), assuming the ground reactions and all other generalized coordinates were well represented by experimental values. Given initial states (i.e., \dot{q}_x , \dot{q}_b , and q_b at $t = 0$), the accelerations were solved at each time step and integrated forward to produce new estimates for pelvis translational (\dot{q}_x^{exp}) and low back angular (\dot{q}_b^{exp}) trajectories. Nonlinear optimization was used to solve for a set of initial states that minimized a cost function:

$$J = \sum_{j=1}^N w_x |\dot{q}_x^{\text{exp}}(jT) - \dot{q}_x^{\text{kin}}(jT)|^2 + \sum_{j=1}^N w_b |\dot{q}_b^{\text{exp}}(jT) - \dot{q}_b^{\text{kin}}(jT)|^2 + \sum_{j=p}^N w_s [|\dot{q}_b^{\text{exp}}(jT) - \dot{q}_b^{\text{kin}}(j-p)T|]^2 \quad (3)$$

which is the weighted sum of the squared deviations from the kinematically determined trajectories plus a penalty term for nonperiodic behavior of the back angles. In Eq. (3), N is the number of data points, T is the sample interval ($= 0.01$ s), p is the number of data points within a half-gait cycle, and w_x , w_b , and w_s are weighting parameters. The optimal pelvis translation and back angle trajectories were then combined with the kinematically determined lower extremity joint angular

trajectories to form a set of generalized coordinate trajectories, \dot{q}^{exp} , to be tracked by the model. The generalized coordinates of the musculoskeletal model were set to q^{exp} to determine the corresponding trajectories of the muscle–tendon lengths ($l_{\text{mt}}^{\text{exp}}$). Both \dot{q}^{exp} and $l_{\text{mt}}^{\text{exp}}$ were subsequently fit with seventh-order splines (Woltring, 1986) prior to tracking.

2.3. Computed muscle control algorithm

CMC was used to compute muscle excitations that would drive a forward dynamic simulation to track the subset of generalized coordinates, \dot{q}_j , corresponding to anatomical joints (Fig. 1):

$$\dot{q}_j = \{q_r^T \ q_1^T \ q_b^T\}^T. \quad (4)$$

Only the anatomical joint angles were tracked since the pelvis (i.e., the base segment) motion is dictated by the foot–floor reactions. At a time t in the simulation, the tracking errors ($\bar{e}_q, \dot{\bar{e}}_q$) between the simulated (\dot{q}_j, q_j) and corresponding experimental states were used to compute a set of desired joint angular accelerations (\ddot{q}^{des}) that should be achieved a short interval ($T = 0.01$ s) later to track \dot{q}_j^{exp}

$$\ddot{q}_j^{\text{des}}(t+T) = \ddot{q}_j^{\text{exp}}(t+T) + k_v[\dot{\bar{e}}_q(t) - \dot{\bar{e}}_q(t)] + k_p[\bar{e}_q(t) - \bar{e}_q(t)], \quad (5)$$

where k_v and k_p are feedback gains for the velocity and position errors, respectively.

Muscle activation and contraction dynamics were integrated forward from t to $t+T$ for a range of muscle

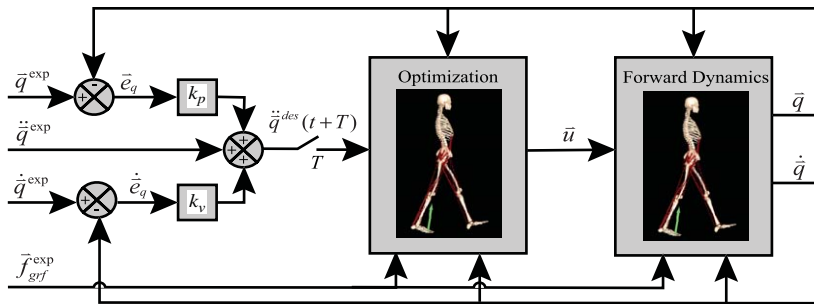


Fig. 1. Schematic of the computed muscle control algorithm applied to gait. The algorithm is applied every $T (= 0.01)$ seconds during a forward dynamic simulation. A set of desired accelerations (\ddot{q}^{des}) are first computed that will drive the generalized coordinates and speeds of the model (\dot{q} and q) toward the experimental kinematics (\dot{q}^{exp} and q^{exp}). k_v and k_p are feedback gains that weight the current velocity ($\dot{\bar{e}}_q$) and position errors (\bar{e}_q), respectively. Static optimization is used to compute a set of desired muscle forces that are achievable at $t+T$, would produce the desired accelerations (\ddot{q}^{des}) in the current configuration, and also minimizes a cost function to resolve muscle redundancy. Muscle excitations (\bar{u}) that produce the desired forces are then found by inverting contraction and activation dynamics. Excitations are held constant while numerical integration of the full system state equations are used to advance all states to $t+T$. The tracking algorithm is applied repeatedly every T seconds until the simulation runs to completion.

excitations ($\vec{0} < \vec{u} < \vec{1}$), with the muscle–tendon lengths during these integrations computed directly from the experimentally derived splines, l_{mt}^{exp} . In this way, the cost of solving the model equations of motion could be avoided at this stage. Forces generated using zero and full excitation provided estimates of the lower ($f_{m,\min}$) and upper ($f_{m,\max}$) bounds on the muscle–tendon forces that could be achieved at $t+T$. Static optimization was then used to compute a set of desired muscle–tendon forces (f_m^{des}) within the range of feasible forces that, when input into the system equations of motion, produce the desired accelerations \vec{q}^{des} and minimize a cost function, J , that resolves muscle redundancy (Happee, 1994):

$$J = \sum_{i=1}^m V_i [a_i(t+T)]^2. \quad (6)$$

In Eq. (6), V_i is the volume of muscle i and $a_i(t+T)$ is the activation of muscle i at $t+T$ corresponding to the desired muscle force, $f_{m,i}^{\text{des}}$. After solving for the desired muscle forces, a root solver was used to determine the muscle excitations (\vec{u}) that, when input into the activation and contraction dynamic equations, would produce the desired muscle forces f_m^{des} . Muscle excitations were then input into the forward dynamic simulation and held constant during integration of the entire set of system state equations from t to $t+T$. The computed muscle control algorithm was repeated every T seconds until the final time of the simulation was reached. The procedures used to obtain the initial values for the muscle–tendon states (i.e., muscle fiber lengths and activations at time $t=0$) are described in the Appendix.

Foot–floor forces during the forward simulation were prescribed to experimental values ($f_{\text{grf}}^{\text{exp}}$), with variations determined by linear translational and rotational spring–dampers applied at the ground reaction center-of-pressure under each foot. The translational spring–damper was applied between the point where the center-of-pressure would act on the foot assuming the experimental generalized coordinates are achieved, and the corresponding location of that point on the foot within the actual simulation. Similarly, rotational spring–dampers were applied in proportion to the difference in orientation between the feet orientations assuming the desired generalized coordinates are achieved and the actual feet orientations. The stiffness and damping of the passive constraints were scaled in and out according to the ratio of body weight supported by each foot.

$$\begin{aligned} \vec{k}_r &= \alpha_r \vec{K}, \\ \vec{k}_l &= [1 - \alpha_r] \vec{K}, \end{aligned} \quad (7)$$

$$\begin{aligned} \vec{b}_r &= \alpha_r \vec{B}, \\ \vec{b}_l &= [1 - \alpha_r] \vec{B}, \end{aligned} \quad (8)$$

where α_r is the ratio of the vertical force under the right foot divided by the total vertical external force, \vec{K} is a 6×1 vector containing three linear (\vec{K}^{lin}) and three rotational (\vec{K}^{rot}) stiffnesses, \vec{k}_r and \vec{k}_l are the current stiffnesses of the springs acting on the right and left foot, respectively, and \vec{B} , \vec{b}_r and \vec{b}_l are the corresponding damping parameters. Important to note is that both the stiffness and damping parameters go to zero when the foot is unloaded so that no force is applied to the foot during swing phase.

2.4. Implementation using experimental gait data

We used the residual elimination and the extended CMC algorithm to generate forward dynamic simulations of a half-cycle of comfortable speed gait for each of 10 young adults (Table 1). For each subject, segment lengths were scaled based on estimated joint-to-joint lengths of the lower extremity and overall subject height. Anthropometric parameters of the musculoskeletal model were estimated based on the subject's total body mass and segment lengths (McConville et al., 1980). Maximum isometric muscle strengths and pennation angles were based on a generic young adult male model (Delp et al., 1990; Carhart, 2000; Anderson and Pandey, 2001). Optimal muscle fiber lengths and tendon slack lengths (Delp et al., 1990; Carhart, 2000; Anderson and Pandey, 2001) were scaled by a ratio of the muscle–tendon length of the scaled model in an upright posture to the corresponding muscle–tendon length of the generic model in the same posture.

The musculoskeletal model and the code describing activation and contraction dynamics were produced using SIMM and the Dynamics Pipeline (Delp and

Table 1
Gait characteristics of the 10 young adults who were included in this study

	Mean (S.D.)
Toe-off (% gait cycle)	61 (1)
Stride length (m)	1.35 (0.11)
Cycle time (s)	1.04 (0.03)
Cadence (steps/min)	115 (4)
Gait speed (m/s)	1.29 (0.10)

Table 2

Parameters used in the residual elimination (REA) and computed muscle control (CMC) algorithms. The residual elimination algorithm weights are used in the computation of the objective function given in Eq. (3), where pelvis translational deviations are measured in mm and low back angular deviations are measured in deg. Position and velocity feedback gains (k_p , k_v) are used in computing the desired joint accelerations (Eq. (5)). Vertical and rotational spring-dampers between the feet and floor were employed to permit variations in ground reactions from experimental values during the forward simulation. The linear and rotation stiffness and damping coefficients for each foot were scaled with the % of body weight support, such that stiffness and damping went to zero during swing (Eqs. (7–8))

Parameter	Description	Value
REA		
w_x	Weight—pelvis translation deviation	1
w_b	Weight—back angle deviation	1
w_s	Weight—back angle symmetry	1
CMC		
k_p	Position error feedback gain	100
k_v	Velocity error feedback gain	20
$\text{---}_{lin} K$	Linear stiffness (N/m) in x , y , z directions	{1000 10000 1000} ^T
$\text{---}_{rot} K$	Rotational stiffness (N m/rad) about x -, y -, z -axes	{500 500 500} ^T
$\text{---}_{lin} B$	Linear damping (N/m s ⁻¹) in x , y , z directions	{20 200 20} ^T
$\text{---}_{rot} B$	Rotational damping (N m/rad s ⁻¹) about x -, y -, z -axes	{20 20 20} ^T

Loan, 2000). Equations of motion for the gait model were derived using SD/FAST (Parametric Technology Corporation, Waltham, MA). All numerical optimizations were performed using a sequential quadratic programming algorithm (FSQP; AEM Design, Tucker, GA). Parameters used in the pre-processing and CMC algorithms are given in Table 2. All computations were done on a personal computer with a 2.2 GHz Pentium processor.

3. Results

The residual elimination algorithm introduced relatively small changes in the pelvis translations. Average root-mean-squared (RMS) differences of less than 5 mm were introduced into the pelvis translations to achieve dynamic balance (Table 3). Slightly larger variations of the low back angles from the kinematically derived values were required to achieve dynamic consistency. Mean RMS differences ranged from 1° in the sagittal plane to 5° in the transverse plane (Table 3). The use of nonlinear optimization to converge to a set of optimal initial states for pelvis translation and low back orientation required about 500 iterations, corresponding to about 10 min of computer processing time.

The CMC algorithm was able to track the experimental joint angles accurately for each subject with only small deviations from the experimental kinematics and ground reaction forces. Mean RMS errors in the lower extremity joint angles ranged from 0.1° to 1.0° over a half-cycle of gait (Fig. 2, Table 4). Mean RMS errors in the ground reaction forces were less than 2 N in the

anterio-posterior and medio-lateral directions, and less than 7 N in the vertical direction (Table 5). The pelvis translations and orientations, despite not being tracked by CMC, remained very similar to experimental values (mean RMS error in translation were <10 mm). The timing of computed muscle activations were all relatively smooth throughout the movement and corresponded closely to published EMG activities of the major lower extremity muscles (Fig. 3). The CMC algorithm required approximately 20 min of computer time to generate each simulation.

4. Discussion

In this study we sought to develop a computationally feasible method for generating forward dynamic simulations of gait that closely track experimental data. We achieved this goal by first using a residual elimination algorithm (REA) to generate a set of desired kinematic trajectories that were dynamically consistent with ground reactions. We then applied a computed muscle control algorithm to determine muscle excitations that drive a forward dynamic simulation to track the desired kinematics. Generating simulations of normal gait from experimental data using this approach required about 30 min (~10 min for the residual elimination algorithm, and ~20 min for the tracking), which is orders of magnitude faster than conventional dynamic optimization approaches. Just as important, these computational benefits were not gained at the expense of tracking accuracy. On the contrary, joint angles were tracked with RMS differences of less than 1°, which is

Table 3

The residual elimination algorithm generated pelvis translation and low back angular trajectories that were dynamically consistent with measured ground reactions. Given are the mean (S.D.) root-mean-squared deviations of these trajectories from the measured kinematics. Note that the back flexion/extension angles were zero-order detrended prior to computing the angular deviations. This allowed for the simulated trajectory to track the pattern of the measured back kinematics, without a penalty being imposed for any constant offset that might be present in the measured low back flexion/extension angle

Pelvis translation (mm)		Low back angle (deg)	
Anterio-posterior	3.3 (1.3)	Flex/extension	0.9 (0.6)
Medio-lateral	1.8 (1.3)	Ad/abduction	2.9 (1.1)
Superior-inferior	4.1 (1.7)	Int/external rotation	4.9 (2.5)

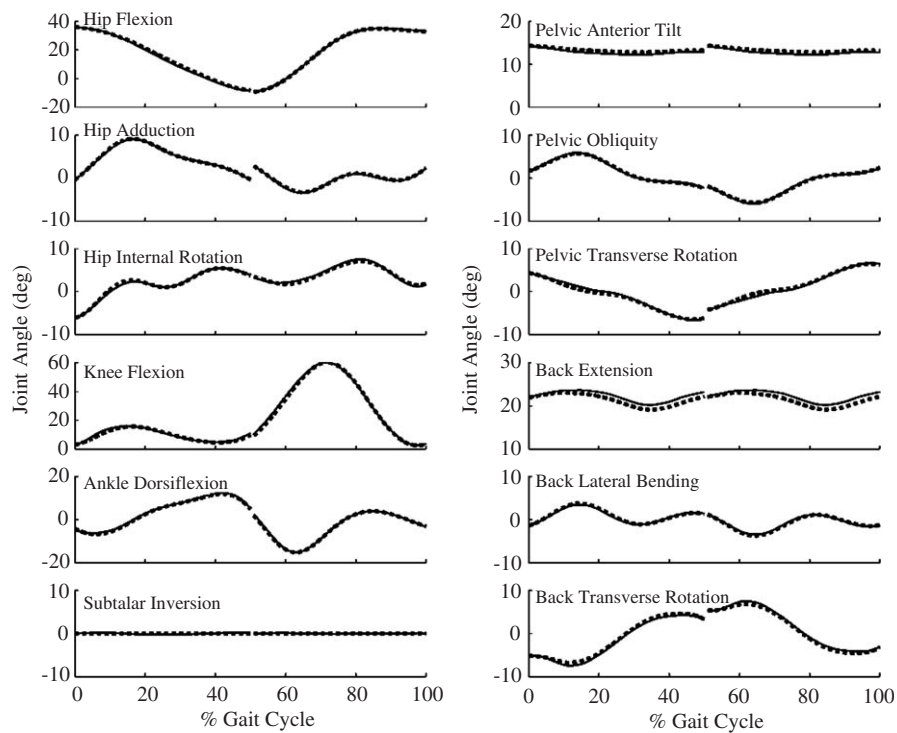


Fig. 2. Simulated joint angles (solid lines) closely tracked experimental values (dashed lines), as demonstrated for one of the subject's gait data. A half-cycle of gait was tracked for each of the subjects. A full cycle of lower extremity joint angles was obtained by juxtaposing the right and left side joint angle trajectories, which created the discontinuities that are evident at 50% of the gait cycle. A zero subtalar angle was tracked since inversion angles were not estimated from the marker set that was used (Davis et al., 1991).

substantially smaller than results obtained using dynamic optimization approaches (Neptune et al., 2001; Anderson and Pandy, 2001).

Forward dynamic simulation permits lines of investigation not available to inverse dynamic techniques (Zajac et al., 2003). Well-established inverse dynamics approaches have been developed for computing and comparing joint kinematics, moments, and powers across subjects (Davis et al., 1991). While these approaches have provided useful information for clinical decision making, they are ultimately limited in that they do not establish cause-and-effect relationships between the underlying elements of the neuromusculoskeletal system and observed kinematics. For example, EMG recordings can indicate when a muscle is active

but cannot explain why a muscle is active or how a muscle contributes to movement. Muscle-actuated forward dynamic simulations bridge this gap by providing a means of estimating the contribution of a muscle to movement (Neptune et al., 2001, 2004) or predicting how movement would be altered as a result of a change to the system or controls (Anderson et al., 2004; Goldberg et al., 2004).

Computed muscle control makes it feasible to use complex, detailed musculoskeletal models when simulating gait without neglecting physiological constraints. The pseudo-inverse method described by Yamaguchi et al. (1995) has been used to simulate gait with complex models (Carhart, 2000) and exhibits fast computational performance, but is limited in that it does not allow

Table 4

Computed muscle control was used to determine muscle excitations that drove the forward simulation to track the experimental joint angles. Given are the mean (S.D.) root-mean-square (RMS) errors between the simulated and experimental quantities over a half-gait cycle

Joint	Direction	RMS error
Pelvis translation	Antero-posterior (mm)	6.3 (1.9)
	Medio-lateral (mm)	0.6 (0.2)
	Vertical (mm)	0.9 (0.4)
Pelvis orientation	Anterior tilt (deg)	0.9 (0.2)
	Obliquity (deg)	0.1 (0.1)
	Internal-external rotation (deg)	0.3 (0.1)
Hip	Flexion-extension (deg)	0.8 (0.2)
	Adduction-abduction (deg)	0.2 (0.1)
	Internal-external rotation (deg)	0.3 (0.1)
Knee	Flexion-extension (deg)	1.0 (0.2)
Ankle	Flexion-extension (deg)	0.3 (0.1)
Subtalar	Inversion-eversion (deg)	0.1 (0.1)
Back	Flexion-extension (deg)	0.6 (0.2)
	Adduction-abduction (deg)	0.1 (0.1)
	Internal-external rotation (deg)	0.3 (0.1)

Table 5

Translational and rotational spring-dampers between the feet and ground allowed the ground reactions the measured values during stance phase. Given are the mean (S.D.) root-mean-square (RMS) errors between simulated and experimental ground reaction forces

Force (N)	RMS error
Antero-posterior	2.2 (0.4)
Medio-lateral	6.5 (2.2)
Vertical	1.0 (0.3)

activation or contraction dynamics to be included in the problem formulation. As a result, unrealistic instantaneous changes in muscle forces can occur, particularly when tracking rapid movements. In contrast, CMC explicitly incorporates activation and contraction dynamics within the problem formulation. Because CMC solutions are excitation driven, CMC allows for changes in excitations to be introduced as a means of assessing how movement might change as a consequence to changes in motor control.

An important component of our approach is the use of the residual elimination algorithm as a pre-processing stage to resolve dynamic inconsistencies between measured kinematics and ground reaction forces. It is not possible to generate a forward dynamic simulation of gait that will simultaneously replicate both measured kinematics and ground reactions without the application of residual forces to the base segment. Other researchers have used this observation to refine anthropometric parameter estimates (Vaughan et al., 1982) and to improve the accuracy of joint moments computed using

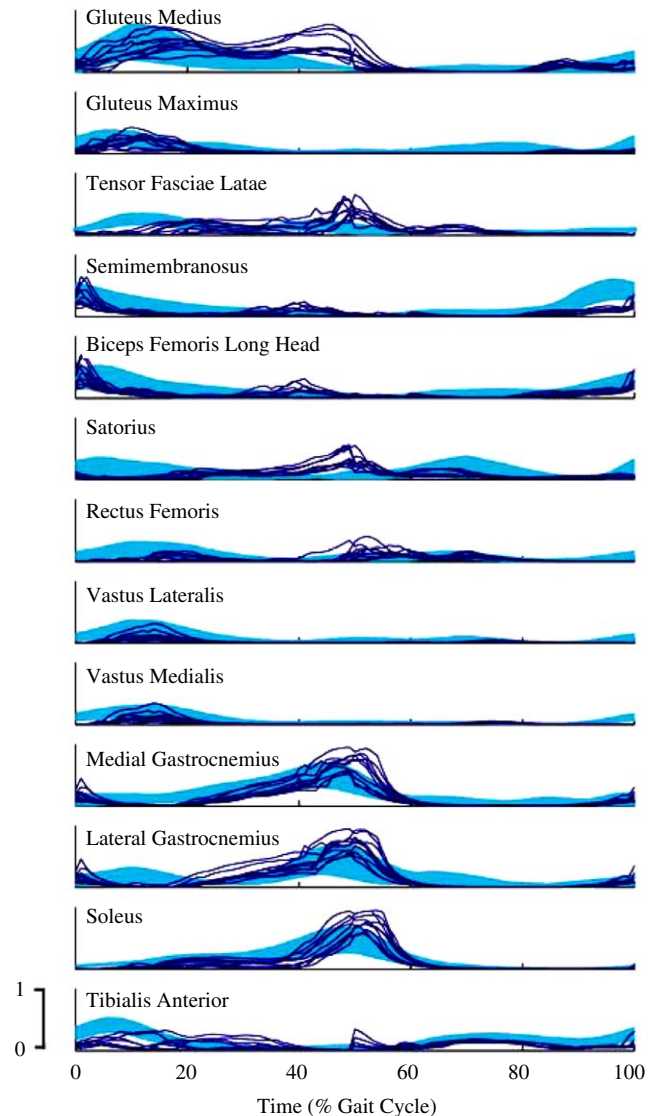


Fig. 3. Estimated muscle activations (solid black lines) for thirteen of the muscles included in the model. Muscle activations over a half-gait cycle from the right and left sides were juxtaposed to create an estimate of activities over a full-gait cycle. Timing of the major muscle activation patterns compare closely with mean (± 1 S.D.) rectified EMG activities (shaded curves) of young adults reported by Winter (1990).

inverse dynamics (Kuo, 1998; Cahouet et al., 2002). Our approach was to compute pelvis translations and low back angles so as to enforce dynamic consistency between kinematics and external forces. Justification for this approach is three-fold. First, the estimation of pelvis orientation and lower extremity joint angles during gait using motion analysis systems is fairly well established and widely used (Davis et al., 1991). Therefore it is desirable to retain this aspect of the movement in any simulation. Second, due to flexibility throughout the torso, the upper body is least well approximated by rigid body assumptions. Consequently, any estimates of representative low back joint angles from kinematic

measures is likely more error prone than lower extremity joint angles. Finally, ground reactions can be very reliably and accurately measured. Thus, the translation of the whole-body motion, as specified by the base segment (pelvis) acceleration, should conform to that dictated by the ground reaction forces. The nominal parameters we used in the residual elimination algorithm ($w_x = w_b = w_s = 1.0$, Table 1) placed equal emphasis on generating pelvis translations and back angles that were consistent with experimental estimates, and back angles that were also cyclically repeating with time. In practice, it would be desirable to select the error weighting parameters based on the variance of noise present in the measured kinematics, when such data is available or can be reliably estimated (Kuo, 1998).

The residual elimination algorithm was capable of fairly quickly converging to a solution that minimally altered measured pelvis kinematics while maintaining a relatively upright posture over a half-gait cycle. The algorithm can be extended for a longer period of time, e.g., a full-gait cycle. However, in practice, we found doing so tended to require larger alterations of the low back angles such that the trunk did not remain as upright. The incorporation of active balance control within CMC, e.g., modulation of foot placement (Bauby and Kuo, 2000), may be needed to simulate a stable upright gait for longer periods of time. Even with a half-gait cycle, exaggerated transverse rotations of the trunk were needed to achieve dynamic balance (Table 3). This likely resulted, in part, from the simplified head–arms–trunk segment which does not model the dynamic contributions of arms to walking (Callaghan et al., 1999) and thus necessitates increased rotation of the rigid upper body to achieve an equivalent dynamic effect. As formulated, the residual elimination algorithm can accommodate models with more detailed representations of the upper body (e.g., inclusion of arms) when such data are available.

The major improvement to the previously employed CMC algorithm (Thelen et al., 2003) is a means of accounting for delays between muscle excitation and active force development. Considering both activation and contraction dynamics, the time constants associated with muscle force development are approximately 10–40 ms during activation and 40–100 ms during relaxation. The slower responses occur in muscles with longer tendons (Zajac, 1989). Such delays in force production can be problematic when solving a tracking problem, particularly during the loading and pushoff phases of the gait cycle when ground reaction forces change rapidly. Our approach to this problem was to anticipate the muscle–tendon forces that could actually be achieved a short time later by integrating the equations for muscle activation and contraction dynamics forward in time. To make these estimates, it was assumed that the muscle–tendon lengths would track

those obtained from experimental joint angles. Note that this assumption was made only when anticipating achievable forces; during the actual forward simulation, the muscle–tendon lengths were computed from the simulated states. While this assumption introduces some error, the feedback components of Eq. (4) were sufficient to correct for these errors. We found that a time window of $T = 0.01$ s produced reasonably smooth muscle excitations and good tracking accuracy. The use of smaller windows tended to introduce substantial fluctuations in muscle excitations (small windows were not long enough to allow muscle forces to change sufficiently), while longer windows resulted in larger tracking errors (greater errors due to substantial changes in the body configuration).

To resolve muscle redundancy, CMC is dependent on a static optimization criterion. In this study, we used the sum of volume-weighted, squared muscle activations (Happee, 1994), but other criteria could be used. For example, a measure of the variation between muscle excitations and measured EMG may be more appropriate for representing the abnormal muscle activation patterns seen in individuals with gait pathologies.

It is important to distinguish tracking approaches, like CMC, from performance-based dynamic optimization of movement (e.g., Anderson and Pandy, 1999). Tracking algorithms determine muscle excitations that closely replicate an observed movement (e.g., Neptune and Hull, 1998). In contrast to this, performance-based dynamic optimization is capable of generating novel movement based on a quantifiable objective (e.g., minimization of metabolic energy during gait (Anderson and Pandy, 2001)), and thus are a powerful means of testing the validity of basic principles that may guide the control of movement. However, due to the nonlinearities of large-scale musculoskeletal models, solving dynamic optimization problems relies heavily on the specification of a good initial estimate to progress to a true optimal solution. In this respect, when a problem necessitates dynamic optimization, efficient tracking algorithms like CMC may be a feasible alternative for generating an initial estimate of the solution.

In conclusion, the speed and accuracy of CMC greatly expand the feasibility of using forward dynamic simulations of gait to investigate muscle function. Future applications include using CMC to generate subject-specific simulations of gait for individuals with movement disorders. Such simulations may prove to be a valuable aid in identifying the underlying causes of a movement disorder and in planning treatment.

Acknowledgements

We gratefully acknowledge the financial support provided by the National Institutes of Health (NIH

grants HD45109, HD38962 and HD33929) and the experimental gait data provided by the Center for Motion Analysis (Connecticut Children's Medical Center).

Appendix

Following are the steps used to set the initial values of the muscle–tendon states (i.e., muscle fiber lengths and activations at time $t = 0$). We extended the experimental kinematic and muscle–tendon length trajectories to negative time assuming that the gait cycle repeats. Muscle activations at a negative time, $t = -0.10$ s, were first set to nominally low levels ($= 0.01$), and the corresponding steady-state muscle fiber lengths and forces were computed (Delp and Loan, 2000). We then used the CMC algorithm to compute constant muscle excitations that, when input into the activation and contraction dynamics equations over the subsequent $T = 0.10$ s, would generate the experimental accelerations, $\ddot{q}^{\text{exp}}(0)$, at $t = 0$. Muscle activations and fiber lengths at $t = 0$ s were then set to the values that resulted from integrating the activation and contraction dynamics using the optimal excitations and the kinematic muscle–tendon length trajectories as inputs from $t = -0.10$ s to $t = 0$ s. The other system states, initial generalized coordinate and speeds, were then set directly to experimental values at time $t = 0$. The CMC algorithm was then used to compute the excitations necessary to track the experimental kinematics from time $t = 0$ forward.

References

- Anderson, F.C., Pandy, M.G., 1999. A dynamic optimization solution for vertical jumping in three dimensions. *Computer Methods in Biomechanics and Biomedical Engineering* 2, 201–231.
- Anderson, F.C., Pandy, M.G., 2001. Dynamic optimization of human walking. *Journal of Biomechanical Engineering* 123, 381–390.
- Anderson, F.C., Pandy, M.G., 2003. Individual muscle contributions to support in normal walking. *Gait & Posture* 17, 159–169.
- Anderson, F.C., Goldberg, S.R., Pandy, M.G., Delp, S.L., 2004. Contributions of muscle forces and toe-off kinematics to peak knee flexion during the swing phase of normal gait: an induced position analysis. *Journal of Biomechanics* 37, 731–737.
- Bauby, C.E., Kuo, A.D., 2000. Active control of lateral balance in human walking. *Journal of Biomechanics* 33, 1433–1440.
- Cahouet, V., Luc, M., David, A., 2002. Static optimal estimation of joint accelerations for inverse dynamics problem solution. *Journal of Biomechanics* 35, 1507–1513.
- Callaghan, J.P., Patla, A.E., McGill, S.M., 1999. Low back three-dimensional joint forces, kinematics, and kinetics during walking. *Clinical Biomechanics* 14, 203–216.
- Carhart, M.R., 2000. Biomechanical Analysis of Compensatory Stepping: Implications for Paraplegics Standing Via FNS. Department of Bioengineering, Arizona State University, Tempe.
- Davis, R.B., Öunpuu, S., Tyburski, D., Gage, J., 1991. A gait analysis data collection and reduction technique. *Human Movement Science* 10, 575–588.
- Delp, S.L., Loan, J.P., 2000. A computational framework for simulation and analysis of human and animal movement. *IEEE Computing in Science and Engineering* 2, 46–55.
- Delp, S.L., Loan, J.P., Zajac, F.E., Topp, E.L., Rosen, J.M., 1990. An interactive graphics-based model of the lower extremity to study orthopaedic surgical procedures. *IEEE Transactions on Biomedical Engineering* 37, 757–767.
- Goldberg, S.R., Anderson, F.C., Pandy, M.G., Delp, S.L., 2004. Muscles that influence knee flexion velocity in double support: implications for stiff-knee gait. *Journal of Biomechanics* 37, 1189–1196.
- Happee, R., 1994. Inverse dynamic optimization including muscular dynamics, a new simulation method applied to goal directed movements. *Journal of Biomechanics* 27, 953–960.
- Kuo, A.D., 1998. A least-squares estimation approach to improving the precision of inverse dynamics computations. *Journal of Biomechanical Engineering* 120, 148–159.
- McConville, J.T., Clauser, C.E., Churchill, T.D., Cuzzi, J., Kaleps, I., 1980. Anthropometric Relationships of Body and Body Segment Moments of Inertia. Wright-Patterson AFB. Air Force Aerospace Medical Research Laboratory, Ohio.
- Neptune, R., 1999. Optimization algorithm performance in determining optimal controls in human movement analyses. *Journal of Biomechanical Engineering* 121, 249–252.
- Neptune, R.R., Hull, M.L., 1998. Evaluation of performance criteria for simulation of submaximal steady-state cycling using a forward dynamic model. *Journal of Biomechanical Engineering* 120, 334–341.
- Neptune, R.R., Kautz, S.A., Zajac, F.E., 2001. Contributions of the individual ankle plantar flexors to support, forward progression and swing initiation during walking. *Journal of Biomechanics* 34, 1387–1398.
- Neptune, R.R., Zajac, F.E., Kautz, S.A., 2004. Muscle force redistributes segmental power for body progression during walking. *Gait & Posture* 19, 194–205.
- Schutte, L.M., Rodgers, M.M., Zajac, F.E., Glaser, R.M., 1993. Improving the efficacy of electrical stimulation-induced leg cycle ergometry: an analysis based on a dynamic musculoskeletal model. *IEEE Transactions on Rehabilitation Engineering* 1, 109–125.
- Thelen, D.G., Anderson, F.C., Delp, S.L., 2003. Generating forward dynamic simulations of movement using computed muscle control. *Journal of Biomechanics* 36, 321–328.
- Vaughan, C.L., Andrews, J.G., Hay, J.G., 1982. Selection of body segment parameters by optimization methods. *Journal of Biomechanical Engineering* 104, 38–44.
- Winter, D.A., 1990. *Biomechanics and Motor Control of Human Movement*. Wiley, New York, NY.
- Woltring, H., 1986. A FORTRAN package for generalized, cross-validatory spline smoothing and differentiation. *Advances in Engineering Software* 8, 104–113.
- Yamaguchi, G.T., Zajac, F.E., 1989. A planar model of the knee joint to characterize the knee extensor mechanism. *Journal of Biomechanics* 22, 1–10.
- Zajac, F.E., 1989. Muscle and tendon: properties, models, scaling, and application to biomechanics and motor control. *Critical Reviews in Biomedical Engineering* 17, 359–411.
- Zajac, F.E., Neptune, R.R., Kautz, S.A., 2003. Biomechanics and muscle coordination of human walking. Part II: lessons from dynamical simulations and clinical implications. *Gait & Posture* 17, 1–17.